EUROPEAN JOURNAL OF CANCER 45 (2009) 3315–3325

available at www.sciencedirect.com

ScienceDirect

journal homepage: www.ejconline.com

Aquaporin-4 contributes to the resolution of peritumoural brain oedema in human glioblastoma multiforme after combined chemotherapy and radiotherapy

Beatrice Nico [a,*], *Domenica Mangieri* [b], *Roberto Tamma* [a], *Vito Longo* [a], *Tiziana Annese* [a], *Enrico Crivellato* [c], *Bianca Pollo* [d], *Emanuela Maderna* [d], *Domenico Ribatti* [a,**], *Andrea Salmaggi* [d]

[a] *Department of Human Anatomy and Histology, Piazza Giulio Cesare, 11, Policlinico I-70124 Bari, Italy*
[b] *Department of Clinical Medicine, Nephrology and Health Sciences, University of Parma Medical School, Parma, Italy*
[c] *Department of Medical and Morphological Research, Section of Anatomy, University of Udine, Medical School, Udine, Italy*
[d] *Foundation IRCCS Neurological Institute 'C. Besta', Milano, Italy*

ARTICLE INFO

Article history:
Received 30 June 2009
Received in revised form 14 September 2009
Accepted 17 September 2009
Available online 14 October 2009

Keywords:
Angiogenesis
Aquaporin-4
Blood–brain barrier
Chemotherapy
Glioblastoma
Radiotherapy
VEGF

ABSTRACT

Brain tumour oedema is coupled with blood–brain barrier damage and alteration in water flow. Aquaporin-4 (AQP4) is involved in the development and resolution of brain oedema, and it is strongly upregulated in glioblastoma multiforme (GBM). Here, we evaluated AQP4 expression and content in GBM and correlated with VEGF–VEGFR-2 expression. In the relapse after chemotherapy and radiotherapy, AQP4 content reduced in parallel with VEGF–VEGFR-2, as compared with primary tumours, and in the peripheral areas of relapsed tumours AQP4 mimicked normal findings of perivascular rearrangement. After immunogold electron microscopy, gold particles were attached on the glial membrane facing the perivascular side, likewise AQP4 gold labelling of the vessels of the control areas. In primary tumours the peripheral vessels appeared faintly marked by AQP4, while the perivascular tumour cells showed a strong expression. The vasculature of the inner tumour areas was unlabelled by AQP4, while tumour cells were labelled, in both primary and relapsing tumours. Relapsed tumours after radiotherapy alone showed slight AQP4 reduction and perivascular restoring in the peripheral areas of the tumour. These data indicate that in GBM chemotherapy and radiotherapy induce a down-regulation in AQP4 expression restoring its perivascular rearrangement suggesting its potential role in the resolution of brain oedema.

1. Introduction

Malignant gliomas are neuroectodermal tumours that commonly arise in the cerebral hemispheres white matter. In humans, gliomas account for 30–45% of all intracranial tumours.[1] Glioblastoma multiforme (GBM) is one of the most highly vascularised tumours, characterised by numerous, abnormal blood vessels, which rapidly proliferate and invade the brain tissue.[2] Tumour blood vessels show several alterations, such as an increased number of endothelial caveolae

* *Corresponding author:* Tel.: +39 080 5478240; fax: +39 080 5478310.
** *Corresponding author.*
E-mail addresses: nico@histology.uniba.it (B. Nico), ribatti@anatomia.uniba.it (D. Ribatti).
0959-8049/$ - see front matter
doi:10.1016/j.ejca.2009.09.023

and fenestrations, prominent pinocytotic vesicles, a lack of perivascular glial endfeet, as well as the opening, loss and/or abnormal morphology of tight junctions, leading to an altered vascular permeability and loss of the blood–brain barrier (BBB) properties.[3–6]

Oedema and the consequent increase in intracranial pressure represent one of the most serious consequences of brain tumour growth,[7] where both vasogenic and cytotoxic oedema are recognisable. Generally, in high-grade gliomas, vasogenic oedema, which drives fluids from blood vessels into the surrounding tissue, is associated with BBB damage, interendothelial tight junction alterations and an increased vascular permeability.[5,8]

Brain water flux is mediated by a specific water channel, named aquaporin-4 (AQP4), which is expressed by perivascular astrocytes endfeet, ependymoglia and glial limitans processes, in both white and grey matters.[9–11] A close relationship between AQP4 and BBB has been demonstrated, because AQP4 is expressed during BBB differentiation[10,12] and has a polarised expression in the perivascular glial processes facing the vessels.[9] In particular, in the Muller cell endfoot membranes facing the vitreous body or blood vessels, AQP4-polarised expression coincides with the localisation of the K^+ channel protein Kir 4.1.[13,14] These findings suggest that AQP4 directs the water flux into the glial compartment and into the vitreous body or vascular compartment, and cooperates in K^+ siphoning at the BBB level. Moreover, studies conducted in AQP4 knock-out mice have shown an important role of AQP4 in oedema development and resolution after ischaemia and water intoxication.[15,16]

Alterations in AQP4 expression have been reported in experimental and pathological conditions, including stroke, brain injuries, muscular dystrophy and tumours, where AQP4 dysregulation is coupled with barrier vessels dysfunction and oedema formation.[17–21] In particular, AQP4, by controlling the bidirectional water flux, is responsible for the formation of cellular brain oedema but counteracts vasogenic oedema.[22] An increased AQP4 expression has been demonstrated in GBM, together with a loss of polarised expression around the vessels and an AQP4 redistribution in glioma cells,[21,23–25] suggesting that increased and/or abnormal AQP4 expression facilitates the oedema fluid flow. Moreover, AQP4 deletion impairs astrocyte migration *in vivo* after injuries, suggesting a role in tumour infiltration.[26]

Vascular endothelial growth factor (VEGF) is involved in promoting both angiogenesis and vascular permeability[27–29] and is upregulated in brain tumours, including GBM.[30,31] The importance of VEGF in regulating tumour angiogenesis, tumour growth and progression has been verified by several reports showing that the inhibition of VEGF/VEGFR-2 by VEGF neutralising antibodies, low-molecular weight VEGFR-2 inhibitors or gene transfer of VEGFR-2 dominant-negative constructs leads to stunted tumour growth with reduced vascularisation.[27] Recently, VEGF has been demonstrated to upregulate AQP4 expression in the ventral midbrain, coupled with BBB leakage and oedema formation.[32]

Combined chemotherapy and radiotherapy is still the most useful post-surgical therapeutic approach in the treatment of GBM and induces significant changes in the functional properties of the blood–brain and blood–tumour barriers.[33,34] In order to investigate the involvement of AQP4 in tumour-related vessel arrangement after chemotherapy and radiotherapy in GBM, in this study we evaluated AQP4 expression and content by immunohistochemistry, immunogold electron microscopy and Western blotting analysis, in surgical specimens obtained from 21 patients affected by GBM and in tumour relapse specimens from the same patients after radiotherapy and chemotherapy treatment and after radiotherapy alone, in both the peripheral and central tumour areas and compared them with AQP4 expression in the peripheral areas distant 1–3 cm from the edge of the tumour, devoid of tumour cells and used as control. Finally, we correlated AQP4 with VEGF–VEGF receptor-2 (VEGFR-2) expression in the same patients, by immunocytochemical and morphometric analysis.

2. Materials and methods

2.1. *Patients and tissue samples*

Surgical specimens from 21 patients operated at the Neurological Institute of Milan and affected by primary GBM were fixed in Carnoy, paraffin-embedded and sectioned at 4 μm. Small pieces of the specimens were also fixed in 0.1 M phosphate-buffered 0.5% glutaraldehyde for immunogold electron microscopic study.

At primary tumour excision, the deep white matter was involved in all cases, and the cortex in five patients. Following the first diagnosis, all patients were treated with standard external beam radiotherapy for a total amount of 60 Gy over 6 weeks. Eighteen patients also underwent a combination of nitrosurea (BCNU) and cis-platinum (CDDP), delivered intravenously every 6 weeks for a median number of six cycles. Three patients underwent only radiotherapy and refused to undergo chemotherapy. At relapse [documented both clinically and by means of Magnetic Resonance Imaging (MRI)], both white matter and cortex were involved in all cases and all patients underwent repeat surgery at the same institution and 18 patients were subsequently treated with second-line chemotherapy and three with loco-regional chemotherapy. Peripheral areas obtained from surgical primary tumours, distant 1–3 cm from the edge of lesion and devoid of tumoural cells were used as control.

2.2. *Determination of peritumoural brain oedema (PTBE) and oedema index (EI)*

The size of the tumour was calculated by multiplying the maximum coronal, axial anteroposterior and axial mediolateral tumour diameters on MRI. The area of PTBE, including the tumour, was obtained using the same model. EI was calculated by dividing the size of the PTBE by that of tumour. All patients were divided into three groups according to the EI as follows: no oedema (EI = 1), moderate oedema (EI = >1) and severe oedema (EI = >2). Additionally, the correlation between EI and the expression levels of AQP4 and VEGF was analysed using univariate analysis and P value < 0.05 was considered significant.

2.3. AQP4 Western blot

Proteins were extracted from histological sections of surgical samples previously fixed in Carnoy buffer and included in paraffin. The sections were deparaffinised and rehydrated in a xylene-graded alcohol scale and the proteins were obtained using a hot lysis buffer (50 mM Tris–HCl, pH 7.5, 150 mM NaCl, 1% NP40, 1 mM phenylmethyllsulfonyl fluoride (PMSF) and a complete protease inhibitor cocktail). Then, 30 μg of total proteins/lane was subjected to 12% sodium docecyl sulphate-polyacrylamide gel electrophoresis (SDS–PAGE) under reducing conditions and then electrotransferred to a polyviyldene fluoride (PVDF) membrane (Millipore Corporate, Billeira, MA, USA). The blots were incubated for 1 h in 5% non-fat dry milk in tris buffered saline tween (TBST), washed in the same buffer and incubated for 2 h at room temperature with a rabbit polyclonal anti-AQP4 antibody used at 1:1000 dilution (Santa Cruz Biotechnology Inc., Santa Cruz, CA, USA) for 2 h at room temperature. Beta-actin protein was detected as control with a mouse anti-beta-actin monoclonal antibody used at 1:500 dilution (Santa Cruz Biotechnology). After four washes in TBST, the membranes were incubated with an anti-rabbit horseradish peroxidase-labelled antibody for AQP4 or with an anti-mouse HPR-labelled-antibody for beta-actin (DAKO Italia, Milan, Italy; Sigma Chemical Co., St Louis, MO, USA). Immunocomplexes were detected using the ECL kit (Santa Cruz Biotechnology) and the blots were exposed to X-ray films, and scanned using Photoshop software (Adobe Systems Inc., San Jose, CA, USA). The intensity of the bands was quantified as arbitrary optical density units using the Scion Image System (based on NIH Image) and expression of AQP4 was normalised to that of the housekeeping protein beta-actin.

2.4. AQP4, VEGF–VEGFR-2 immunocytochemistry

Four μm histological sections collected on poly-L-lysine-coated slides (Sigma Chemical Co.) were deparaffinised and stained with a three-layer avidin–biotin-immunoperoxidase technique. The sections were rehydrated in a xylene-graded alcohol scale and then rinsed for 10 min in 0.1 M phosphate-buffered saline (PBS). The sections were treated with 0.1% trypsin (Sigma Chemical Co.) in $CaCl_2$ 0.01 M for 30 min at room temperature and then exposed to anti-AQP4, anti-VEGF-A and anti-VEGFR-2 primary antibodies (Santa Cruz Biotechnology Inc.) diluted 1:100 in RPMI-1640 medium supplemented with 10% heat-inactivated foetal calf serum (FCS) overnight at 4 °C. The sections were then incubated with biotinylated swine anti-rabbit Ig (Dako) diluted 1:300 in RPMI-1640 supplemented with 10% heat-inactivated FCS for 15 min at room temperature, and streptavidin-peroxidase conjugate (Vector Laboratories, Burlingame, CA, USA) diluted 1:250 in PBS for 15 min at room temperature. Immunodetection was performed in 0.05 M acetate buffer, pH 5.1, 0.02% 3-amino-9-ethylcarbazole grade II (Sigma Chemical Co.) and 0.05% H_2O_2 for 20 min at room temperature. Afterwards, the sections were washed in the same buffer and counterstained with Gill's haematoxylin (Polysciences, Warrington, PA, USA), and mounted in buffered glycerine. A preimmune rabbit serum (DAKO Italia) replacing the primary antibody served as a negative control. The sections were then examined with an Olympus photomicroscope (Olympus Italia, Rozzano, Italy) and digital images were obtained with a cooled CCD camera (Princeton Instruments, Princeton, NJ, USA).

2.5. Morphometric analysis of AQP4 and VEGF–VEGFR-2 expressions

Morphometric analysis was performed on nine randomly selected fields every three sections, obtained from biopsy specimens of the primary and relapsed tumoural tissues of each patient, observed at ×400 magnification with an Olympus photomicroscope, using Image Analysis software (Olympus Italia). AQP4 and VEGF/VEGFR-2 labelled areas were evaluated. The mean value in each image from the section, the final mean value for all the images and the standard error of the mean (SEM) were calculated. The statistical significance of the differences between the mean values of the labelled area between primary and relapsed tumours was determined by Student's *t* test with GraphPad Prism 3.0 software (GraphPad software, La Jolla, CA, USA). The findings were considered significant at P values <0.05.

2.6. Immunogold electron microscopy

Small pieces of the specimens were fixed in a 0.1 M phosphate-buffered mixture of 0.1% glutaraldehyde for 30 min at 4 °C and then rinsed with 10 mM ammonium chloride in 0.1 M (PBS) for 45 min. The samples were dehydrated in an ascending ethanol series and embedded in the acrylic resin LR-Gold (London Resin Co., Reading, UK) with 0.8% benzil. The resin was hardened at –25 °C under the light of a halogen lamp (500 W). Thin sections were cut with an LKB V ultramicrotome and collected on formvar-coated nickel grids. The grids were incubated for 10 min at room temperature with PBS buffer. Unspecific reactions were blocked with 1% BSA–PBS, pH 7.4, for 10 min, at room temperature. The sections were incubated with the primary anti-AQP4 antibody diluted 1:50 in PBS at room temperature overnight, washed with PBS and incubated for 1 h at room temperature with the second antibody (goat anti-rabbit) coupled to 6–30 nm gold particles (Chemicon Int. Inc., Temecula, CA, USA). After washing with PBS, the grids were stained with 1% uranyl acetate, followed by 1% lead citrate and examined with a Zeiss EM 109 electron microscope (Zeiis, Oberkochen, Germany) and digital images were obtained with a cooled camera Gatan CMS (Gatan GmbH, München, Germany).

2.7. Quantification of the perivascular AQP4 gold particles distribution

To quantify the AQP4 gold particles distribution on the perivascular glial endfeet, 40 electron micrographs at the final magnification of ×20,000 were randomly chosen from three patients for each of the following condition: (i) peripheral areas of primary tumours, distant 1–3 cm from the edge of the lesion, devoid of tumoural cells used as control; (ii) peripheral areas of primary tumours containing tumour cells; (iii) peripheral areas of chemotherapy and radiotherapy-treated relapsed specimens and (iv) peripheral areas of radiotherapy-treated relapsed specimens. The total number

of gold particles distributed along the length of the abluminal microvessel sides (glial endfeet membranes) was counted with the use of an electronic pen connected to a graphic tablet (Digicad Plus, Kontron Elektronic, GMBH, Germany) and to a VIDAS 2.5 computerised image analyser (Kontron Elektronic). The results were expressed as the number of gold particles per μm of microvessels on abluminal front. The mean value in each micrograph, the final mean value for all the micrographs of each patient and of the all the patients in each condition and the SEM were calculated. The statistical significance of the differences between the mean values of the number of gold particles between primary and relapsed tumours was determined by Student's *t* test with GraphPad Prism 3.0 software (GraphPad software). The findings were considered significant at P values < 0.05.

3. Results

3.1. *Western blotting*

Immunoblotting analysis of AQP4 protein in surgical homogenates showed a higher protein expression in primary tumours than in chemotherapy and radiotherapy-treated relapsed tumours (Fig. 1A). Densitometric analysis confirmed that in relapsed tumours AQP4 decreased by 69% as compared to primary tumours (Fig. 1B).

3.2. *Immunocytochemical expression and quantification of AQP4 in the tumour central area*

In the central areas of surgical specimens, with the exception of the necrotic area, of both primary and relapsed tumours, marked hypercellularity, nuclear atypia, frequent mitoses and aberrant vasculature were observed. No difference in AQP4 expression and content was detected in these areas between primary and relapsed tumours. Loss of perivascular AQP4 polarity and its redistribution on the plasmamembrane and cytoplasm of the tumour cells were detectable (Fig. 2C–G). Moreover, the vessels showed an extremely irregular course, often featuring a glomeruloid aspect with hyperplastic wall (Fig. 2C, D and G) lacking in AQP4-labelled perivascular glial processes, and were surrounded by plasmamembranes of tumour cells strongly labelled by AQP4 (Fig. 2C, E–G). Morphometric analysis showed no significant differences in AQP4 labelling in the central area between primary and relapsed tumours (Fig. 5). On the contrary, in the brain areas used as controls, the vessels showed a thin wall uniformly stained by AQP4 (Fig. 2A) and labelled glial processes forming a continuous perivascular sheath were detected (Fig. 2B).

3.3. *Immunocytochemical expression and quantification of AQP4 in the tumour peripheral area*

The peripheral areas of surgical specimens of primary tumours were characterised by a decreased tumour cell density as compared with the inner areas, by apparently normal glial cells and reactive hypertrophic astrocytes. Thickened vessels lightly labelled by AQP4 (Fig. 3A), or unlabelled vessels often connected with cytoplasmic protrusions of adjacent tumour

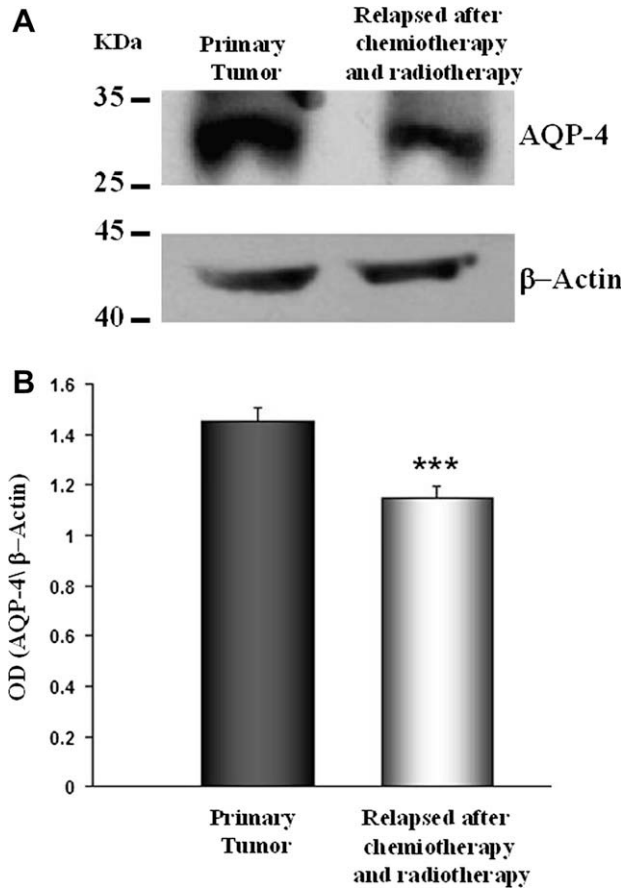

Fig. 1 – AQP4 expression in GBM biopsy specimens from primary and chemotherapy and radiotherapy-treated relapsed tumours. (A) Western blot for AQP4 of the total protein extract from the biopsies. (B) Quantification of AQP4 after Western blot analysis. The histograms show a significant reduction in AQP4 in the treated relapsed biopsies compared with the primary tumour specimens (1.03 ± 0.1 versus 1.44 ± 0.03. $P < 0.001$). The error band represents the SEM of 10 experiments. OD = optical density.

cells, strongly expressing AQP4 in both the cytoplasm and plasmamembrane (Fig. 3A, inset) were detected.

In the peripheral areas of surgical specimens of relapsed tumours from patients treated with chemotherapy and radiotherapy, numerous vessels with a perivascular arrangement of AQP4 (Fig. 3C and E), forming a continuous labelled layer on the abluminal side (Fig 3E) and surrounded by bodies and processes of labelled astrocytes (Fig. 3D), were recognisable.

Differently, the peripheral areas of surgical specimens of relapsed tumours from patients treated with radiotherapy alone were similar to the primary tumour specimens, in terms of AQP4 expression. The vessels appeared only faintly labelled, or completely unlabelled by AQP4 and were enveloped by markedly labelled tumour cells (Fig. 3B). Morphometric analysis showed a significantly reduced AQP4 expression in the peripheral areas of surgical specimens from relapsed tumours treated with chemotherapy and radiotherapy as compared to primary tumours and to specimens from relapsed tumours treated with radiotherapy alone, while no significant AQP4 reduction was detected in the peripheral areas

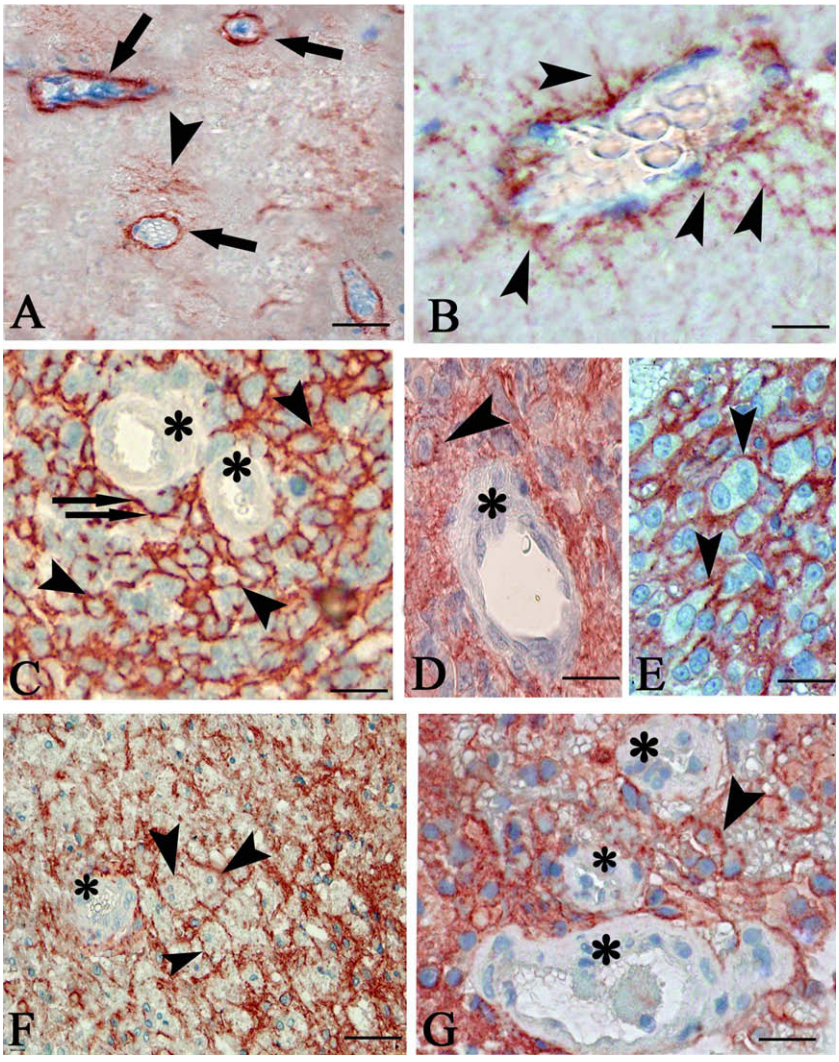

Fig. 2 – AQP4 immunocytochemical localisation in control brain specimens (A and B), in the central areas of GBM primary surgical specimens (C, D and E), in relapsed surgical specimens from patients treated with radiotherapy (F) and with chemotherapy and radiotherapy (G). (A and B) AQP4 uniformly stains vessels (A, arrows), glial processes in the neuropile (A, arrowhead) and forms a continuous perivascular sheath (B, arrowheads). (C–G) AQP4 is strongly redistributed on the tumour cell glial membranes (C–G, arrowheads), while vessels show unlabelled hyperplastic walls (C, D, F and G asterisks), surrounded by intensely marked glioma cells (C, double arrows). No significant differences in AQP4 labelling are recognised between primary and relapsed tumours. Scale bar: A, C, F, 50 μm; B, D, G, 25 μm; E, 16.6 μm.

of biopsy specimens from relapsed tumours treated with radiotherapy alone, as compared to primary tumours (Fig. 5).

3.4. *Immunogold electron microscopy*

In control specimens, numerous AQP4 gold particles were recognisable on the plasmamembranes of the astrocyte processes enveloping the vessel wall (Fig. 4A, Table 1). On ultrathin sections of the peripheral areas of the primary tumour specimens, the vessels showed few AQP4 gold particles on their abluminal side, while the tumour cells displayed numerous gold particles attached on the plasmamembrane and scattered in the cytoplasms (Fig. 4B, D and E, Table 1). In the peripheral areas of surgical specimens of relapsed tumours from patients treated with radiotherapy alone no difference in the vessels labelling was observed as compared with primary tumour specimens. In fact, isolated AQP4 gold particles on the abluminal side of the irregularly arranged vessels were recognisable (Fig. 4C, Table 1). On the contrary, in the peripheral areas of surgical specimens of relapsed tumours from patients treated with chemotherapy and radiotherapy, the vessels showed many gold particles on the glial membranes facing the vessels, as in the control specimens (Fig. 4F and G, Table 1).

3.5. *Immunocytochemical expression and quantification of VEGF–VEGFR-2*

In order to evaluate whether the alterations in AQP4 expression could be correlated to an increased angiogenesis and

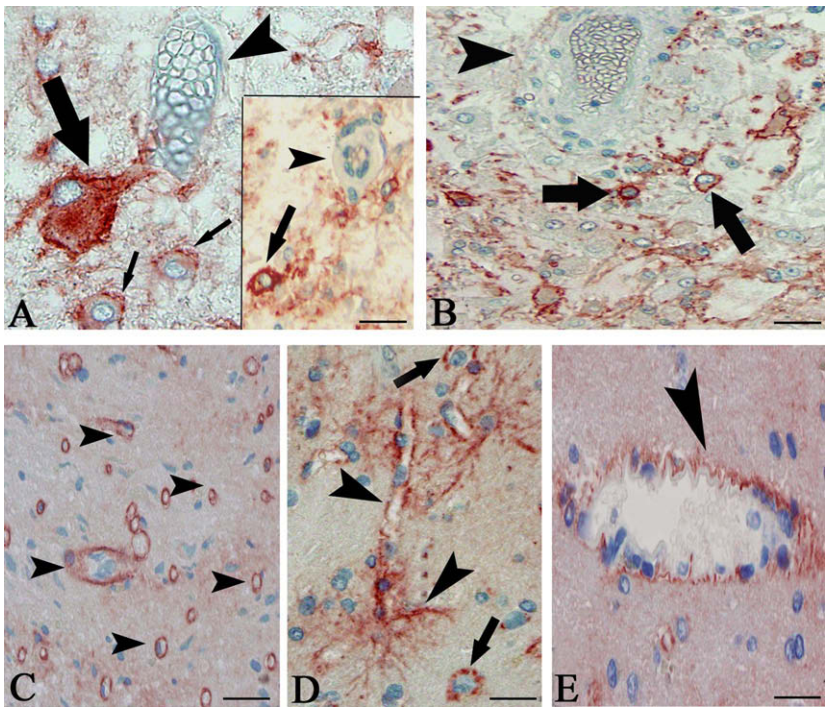

Fig. 3 – AQP4 immunocytochemical localisation in the peripheral areas of GBM primary surgical specimens (A), in relapsed surgical specimens from patients treated with radiotherapy (B) and with chemotherapy and radiotherapy (C–E). (A) Primary tumour shows a vessel faintly labelled by AQP4 (arrowhead), surrounded by tumour cells expressing AQP4 on the membranes (thin arrows) and connected with a cytoplasmic extension of an adjacent tumour cell, strongly expressing AQP4 in both the cytoplasm and plasmamembrane (thick arrow). Note in the inset, an AQP4-labelled tumour cell (arrow) near to an unlabelled, thick vessel wall (arrowhead). (B) A faintly AQP4-labelled vessel (arrowhead) is surrounded by stained tumour cells (arrows). (C–E) Numerous thin walled vessels with a continuous AQP4 perivascular arrangement (arrowheads) are surrounded by astrocytes-labelled processes (D, arrowheads) and by a few tumour cells, with stained plasmamembranes (D, arrows). Compare the AQP4 vessels staining of the panels C and E, with the panels A and B of Fig. 2. Scale bar: A, D, E, 25 μm; C, 50 μm; B, 33.3 μm.

vascular permeability, we analysed VEGF–VEGFR-2 expression in biopsy specimens of primary tumours after chemotherapy and radiotherapy. VEGF was strongly expressed by tumour and endothelial cells in the central areas of both primary and relapsed tumours, (Fig. 6A and B), whereas it was faintly expressed in the peripheral areas of both tumour and endothelial cells (Fig. 6C). No vessels labelling was detected in the peripheral area of the relapsed tumours, which showed few VEGF-labelled tumour cells around the vasculature (Fig. 6D).

As concerns VEGFR-2 expression, both tumour and endothelial cells were strongly reactive in the central areas of the primary and relapsed tumours (Fig. 7A and B). In the peripheral areas, instead, endothelial and tumour cells were strongly labelled only in the primary tumours (Fig. 7C), whereas in the relapsed tumours only tumour cells near the vessels were labelled, whereas endothelial cells appeared only faintly labelled or unlabelled (Fig. 7D). Morphometric analysis demonstrated in peripheral tumour areas a significant reduction of VEGF–VEGFR-2 labelling in relapsed tumours after combined chemotherapy and radiotherapy as compared to primary tumours (Fig. 8).

3.6. *AQP4 and VEGF expressions correlate with brain oedema*

AQP4 and VEGF expressions in peritumoural area correlate with EI ($P < 0.05$) in primary tumours, as well as in relapsed tumour after radiotherapy and after chemotherapy and radiotherapy. In general, higher AQP4 and VEGF expression values were associated with higher EI values (>2).

4. Discussion

In this study we have demonstrated that in relapsed GBM, after chemotherapy and radiotherapy, a significant reduction of the AQP4 content and its perivascular rearrangement are detectable, whereas in relapsed tumours after radiotherapy alone, no significant AQP4 reduction or perivascular rearrangement is observed. Moreover, our results suggest that the vasogenic oedema occurring in GBM might be a consequence of an increased vascular permeability and a loss of polarised AQP4 expression on the perivascular side. In this context, AQP4 redistribution taking place in GBM could be seen as a cellular reaction to the excess influx of interstitial

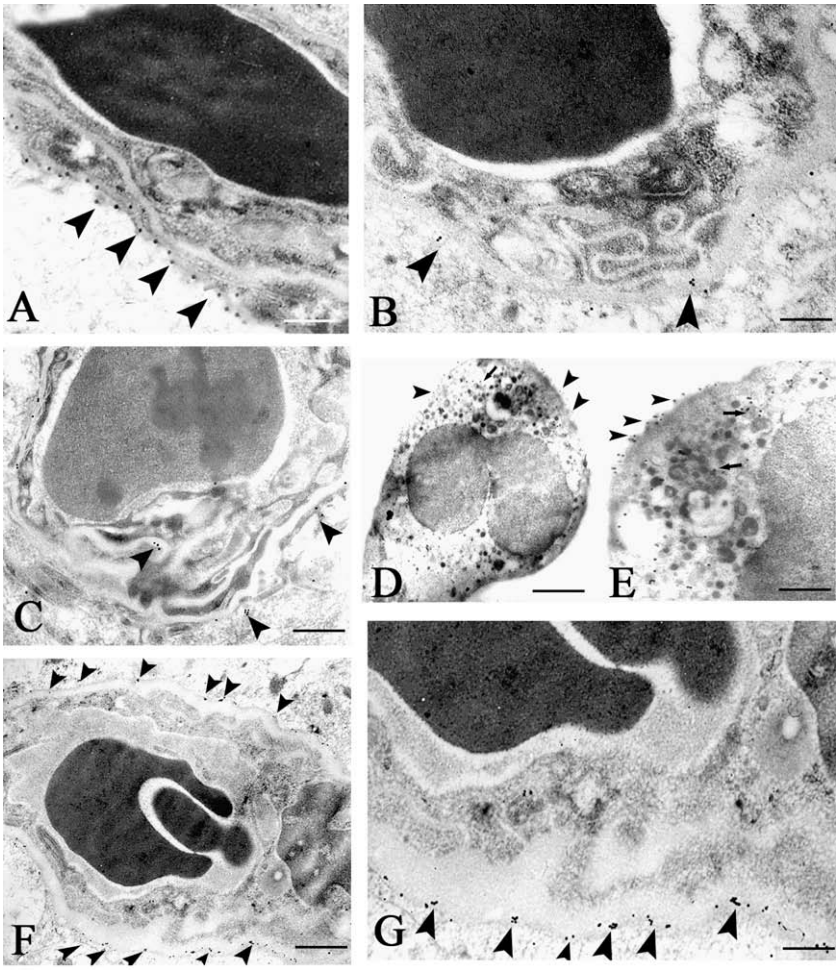

Fig. 4 – AQP4 ultrastructural immunolocalisation in the peripheral areas of control brain specimens (A), in the peripheral areas of GBM primary surgical specimens (B), of relapsed surgical specimens from patients treated with radiotherapy (C–E) and with chemotherapy and radiotherapy (F and G). Numerous AQP4 gold particles (arrowheads) are attached on the abluminal side of a vessel in control brain specimen (A), while few number of particles are present on the abluminal vascular side in primary tumour specimen (B) and in tumour specimens from patients treated with radiotherapy (C–E), where gold particles are present also on the plasmamembranes (D and E, arrowheads) and scattered in the cytoplasm of tumour cells (D and E, arrows). In tumour specimens from patients treated with chemotherapy and radiotherapy, numerous AQP4 particles decorate the perivascular glial membranes (F and G, arrowheads).Compare the panel G with the panel A. Scale bar: A, B, G, E, 0.5 μm; C, D, F, 0.8 μm.

fluid in the altered BBB, and AQP4 seems to play a crucial role in the dynamic of the resolution of brain oedema in GBM and may be considered a useful marker to evaluate the positive effects of chemotherapy and radiotherapy administered in combination.

Another interesting data of this study concern a difference in the expression of AQP4 between the central and peripheral areas of the tumours. In fact, in the peripheral areas of relapsed tumours after chemotherapy and radiotherapy, AQP4 expression restores a normal perivascular rearrangement, unlike the peripheral areas of primary tumours, where vessels appear unlabelled or faintly stained for AQP4 and the tumour cells are strongly reactive to AQP4. Moreover, in the central areas of both primary and relapsed tumours after chemotherapy and radiotherapy the vessels are unlabelled by AQP4 and the tumour cells are intensely labelled, while in relapsed tumours after radiotherapy alone, no significant AQP4 reduction and perivascular rearrangement were observed.

In GBM, the peritumoural vessels showed an increased vascular permeability and maintained some of the BBB characteristics, such as ZO-1-associated tight junction proteins and a basal lamina.[5,35,36] Moreover, the vessels are surrounded by agrin and AQP4 colocalises with alpha-dystroglycan suggesting that the extracellular matrix determines astrocytes polarity through the binding to alpha-dystroglycan, which, in turn, is responsible for the ability of astrocytes to induce barrier properties in endothelial cells.[23,24] Our results indicate that peripheral tumoural vessels could have different molecular features as compared to inner vessels, and in accordance with the previous studies[23–25,31] suggest that peritumoural oedema might be caused by the loss of the perivascular arrangement of AQP4, indicating a protective role of

Table 1 – Quantitation of AQP4-labelled gold particles distribution on the perivascular membranes in controls and from surgical specimens of primary tumours, and relapsed after radiotherapy and combined chemotherapy and radiotherapy.

	No. of vessels	No. of gold particles/μm of abluminal microvessel length
Control	30	25 ± 3
Primary tumours	30	3 ± 0.2*
Relapsed after radiotherapy	30	2.6 ± 0.1*
Relapsed after chemotherapy and radiotherapy	30	32 ± 7

Values represent the mean ± SEM of 40 electron micrographs at a final magnification of ×20,000 for each control and tumour specimen examined.

* $P < 0.0001$ versus control.

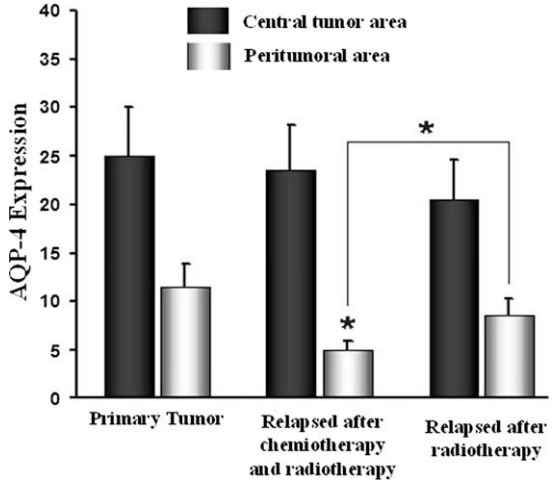

Fig. 5 – Morphometric assessment of AQP4 expression. Morphometric analysis shows no significant differences in AQP4 expression in the central areas between primary and relapsed tumours. On the contrary, AQP4 expression in the peripheral areas of specimens from relapsed tumours treated with chemotherapy and radiotherapy as compared to primary tumours and to specimens from relapsed tumours treated with radiotherapy alone is significantly reduced, while no significant AQP4 reduction is detected in the peripheral areas of biopsy specimens from relapsed tumours treated with radiotherapy alone, as compared to primary tumours.*$P < 0.05$ versus primary tumour and versus relapsed tumours treated with radiotherapy alone.

AQP4 in counteracting oedema formation. Tumour-associated oedema is the cause of significant morbidity in GBM and a balance must be achieved between restoring BBB to reduce oedema and maintaining a permeable BBB to allow penetration of chemotherapy agents. Corticosteroids are largely used in combination with chemotherapy and contribute to significantly reduced peritumoural brain oedema by decreasing the permeability of tumour vessels and/or enhancing the clearance of extracellular water.[37] Moreover, corticosteroids reduced both VEGF expression and AQP4 mRNA level in experimental brain tumour model and after intracerebral haemorrhage in rats.[38,39] A protective role for AQP4-polarised induction has been demonstrated also against post-ischaemic oedema and BBB disruption.[40,41]

In GBM, AQP4 co-localisation with K^+ channel protein Kir 4.1[14] is abolished[24] and a mislocation of Kir channels, coupled with a lack of Kir in glioma cells has been reported,[42] suggesting that AQP4 anchoring to glial membranes is necessary to cooperate in K^+ siphoning. A redistribution of both AQP4 and Kir 4.1, as well as of alpha-1 syntrophyn, has been described in GBM,[23,24] suggesting that these molecular rearrangements occur as a reaction to vasogenic oedema, to facilitate oedema resolution.

AQP4 is also involved in astrocyte migration,[43,44] which is delayed in AQP4 null mice.[44] Experimental data suggest a link between glioma cell invasive capacity and glioma-associated angiogenesis.[45] Here, we have observed in the peripheral areas of primary tumours isolated glioma cells strongly labelled by AQP4, indicative of their migratory activities. Glioma cells show cytoskeleton alterations and a rearrangement of actin filaments[46] and it may be hypothesisable that cytoskeleton alterations occurring during glioma transformation induce an up-regulation and mislocalisation of AQP4, favouring tumour cells detachment and migration.

An increase in VEGF–VEGFR-2 immunoreactivity has been reported in both tumour and endothelial cells, and it correlates with malignancy grade and displays a spatial-temporal correlation with angiogenesis in GBM.[47–49] Moreover, the role of VEGF in the breakdown of the BBB in GBM, leading to peritumoural vasogenic oedema, is also well recognised and a close relationship exists between VEGF–VEGFR-2 and AQP4 expressions in brain tumours.[50] Accordingly to this latter, we have demonstrated that an increased VEGF–VEGFR-2 expression is coupled with an altered expression of AQP4 and brain oedema in dystrophic mdx mice[26,28,29] and intracerebral injection of VEGF induces an up-regulation of AQP4 expression associated with BBB disruption.[32] Here, we have demonstrated that in relapsed GBM specimens obtained from patients after combined chemotherapy and radiotherapy, as compared with primary tumour specimens, AQP4 expression is reduced and restores perivascular arrangement in the peripheral tumour areas, together with a decreased VEGF–VEGFR-2 expression.

The normally polarised rearrangement of AQP4 in peripheral areas in tumour specimens obtained after combined chemotherapy and radiotherapy could be expression of a process of normalisation of tumour blood vessels. In fact, tumour vasculature is structurally and functionally abnormal and blood vessels are leaky, tortuous, dilated, pericytes are loosely attached or absent and the basement membrane is often

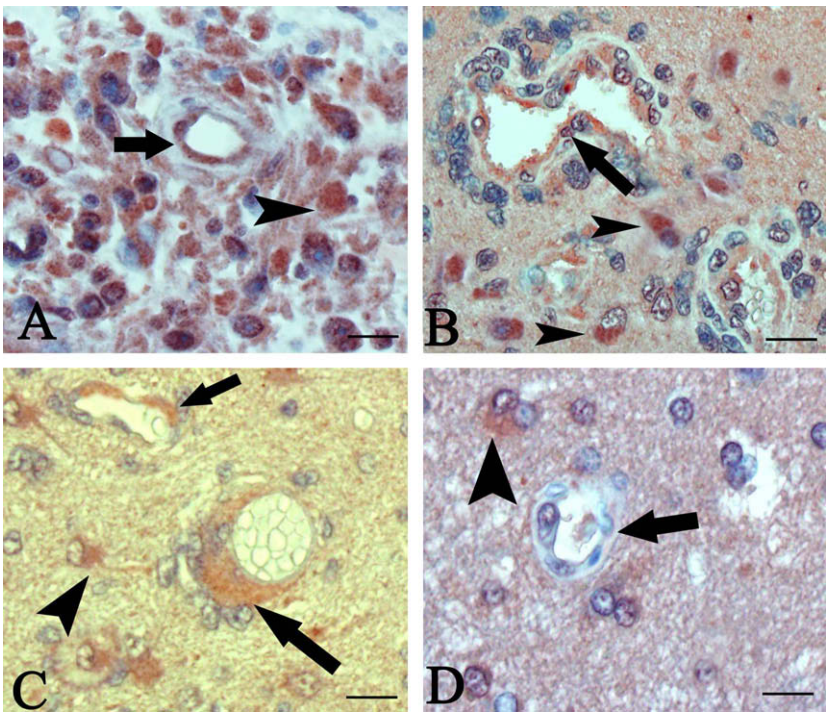

Fig. 6 – Immunocytochemical expression of VEGF in primary (A and C) and in relapsed specimens from patients treated with chemotherapy and radiotherapy (B and D). (A and B) tumour cells (arrowheads) and endothelial cells (arrow) strongly express VEGF in the central areas of primary (A) and relapsed tumours (B). (C and D) VEGF staining is present in both tumour (C, arrowhead) and endothelial cells (C, arrows) in the peripheral areas of primary tumour. No endothelial labelling is present in relapsed tumours (D, arrow), showing perivascular tumour cells (D, arrowhead) faintly labelled by VEGF. Scale bar: A–D, 25 μm.

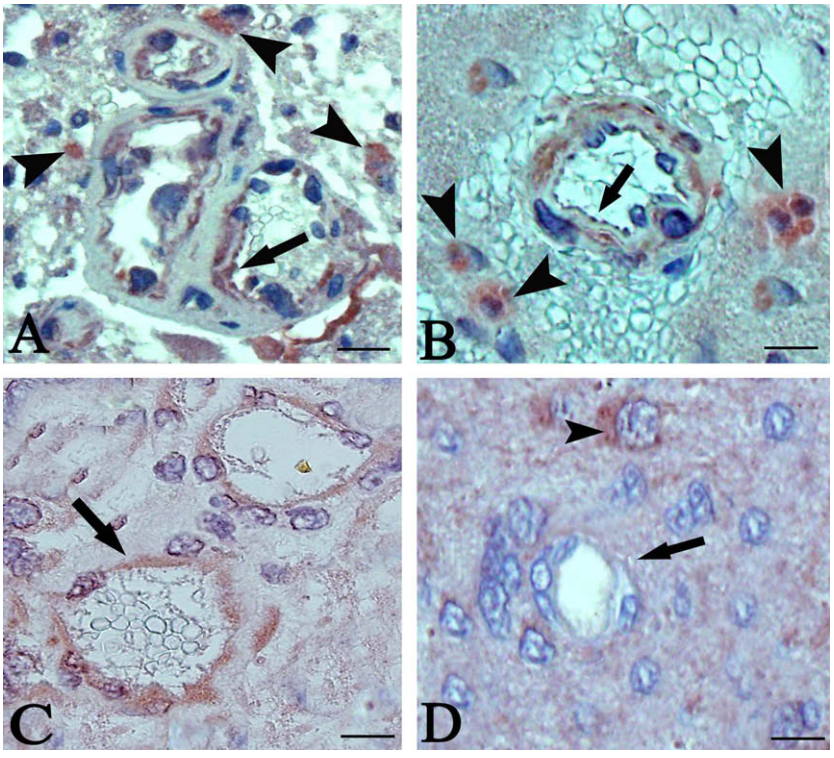

Fig. 7 – Immunocytochemical expression of VEGFR-2 in primary (A and C) and in relapsed specimens from patients treated with chemotherapy and radiotherapy (B and D). (A and B) Tumour (A and B, arrowheads) and endothelial cells (A and B, arrows) are strongly labelled by anti-VEGFR-2 antibody in the central areas of primary (A) and relapsed tumours (B). (C and D) Peripheral areas show strongly labelled endothelial cells in primary tumour (C, arrow), and few labelled tumour cells (D, arrowhead) near to unlabelled endothelial cell (D, arrow) in the relapsed tumour. Scale bar: A–D, 25 μm.

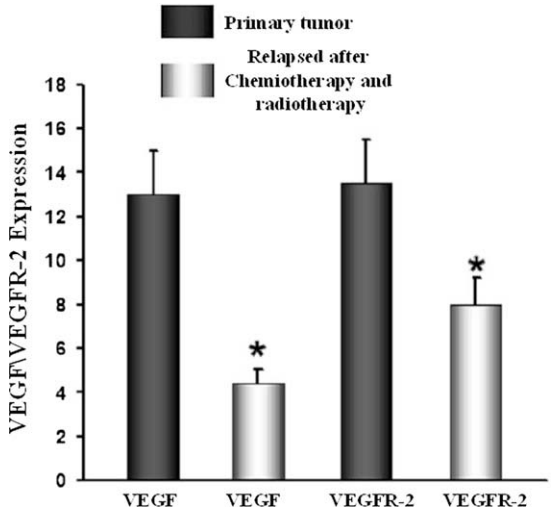

Fig. 8 – Morphometric assessment of VEGF and VEGFR-2 expressions. Morphometric analysis demonstrates in peripheral tumour areas a significant reduction of VEGF–VEGFR-2 labelling in relapsed tumours after combined chemotherapy and radiotherapy as compared to primary tumours. $P < 0.001$ versus primary tumours.

abnormal. One of the aims of the antiangiogenic therapy in the treatment of tumours is to obtain their normalisation: the normalised vasculature is characterised by vessels that are less leaky, dilated and tortuous than abnormal vessels, with a basement membrane and covered by pericytes.[51]

Overall, in this study we have demonstrated that in relapsed GBM specimens obtained from patients after combined chemotherapy and radiotherapy, AQP4 content and VEGF–VEGFR-2 expression are significantly reduced as compared with primary tumour specimens. These data suggest that combined chemotherapy and radiotherapy induces a down-regulation of AQP4 expression and restores a normally polarised rearrangement of AQP4 in the peripheral tumour areas, coupled with a reduction in VEGF–VEGFR-2 expression, and suggest a potential role for AQP4 in the resolution of brain oedema.

Conflict of Interest statement

None declared.

Acknowledgements

This study was supported in part by grants from MIUR (PRIN 2007), Rome, and the Fondazione Cassa di Risparmio di Puglia, Bari, Italy. The authors would also like to thank M.V.C. Pragnell, B.A., for linguistic revision.

REFERENCES

1. Kleinhues P, Cavanee W. *Astrocytic tumors. Pathology and genetics of tumors of the nervous system World Health Organization classification of tumors*. Basel: ISN Neuropathol Press; 2000. p. 9–52.
2. Brat DJ, Castellano-Sanchez A, Kaur B, Van Meir EG. Genetic and biologic progression in astrocytomas and their relation to angiogenic dysregulation. *Adv Anat Pathol* 2002;**9**:24–36.
3. Nir I, Kohn S, Doron Y, Israel O, Front D. Quantitative analysis of tight junctions and the uptake of 99mTc in human gliomas. *Cancer Invest* 1986;**4**:519–24.
4. Dinda AK, Sarkar C, Roy S, et al. A transmission and scanning electron microscopic study of tumoral and peritumoral microblood vessels in human gliomas. *J Neurooncol* 1993;**16**:149–58.
5. Liebner S, Fischmann A, Rascher G, et al. Claudin-1 and claudin-5 expression and tight junction morphology are altered in blood vessels of human glioblastoma multiforme. *Acta Neuropathol* 2000;**100**:323–31.
6. Rascher G, Fischmann A, Kröger S, Duffner F, Grote EH, Wolburg H. Extracellular matrix and the blood–brain barrier in glioblastoma multiforme: spatial segregation of tenascin and agrin. *Acta Neuropathol* 2002;**104**:85–91.
7. Marmarou A. A review of progress in understanding the pathophysiology and treatment of brain edema. *Neurosurg Focus* 2007;**22**:E1.
8. Wolburg H, Wolburg-Buchholz K, Kraus J, et al. Localization of claudin-3 in tight junctions of the blood–brain barrier is selectively lost during experimental autoimmune encephalomyelitis and human glioblastoma multiforme. *Acta Neuropathol* 2003;**105**:586–92.
9. Nielsen S, Nagelhus EA, Amiry-Moghaddam M, Bourque C, Agre P, Ottersen OP. Specialized membrane domains for water transport in glial cells: high-resolution immunogold cytochemistry of aquaporin-4 in rat brain. *J Neurosci* 1997;**17**:171–80.
10. Nico B, Frigeri A, Nicchia GP, et al. Role of aquaporin-4 water channel in the development and integrity of the blood–brain barrier. *J Cell Sci* 2001;**114**:1297–307.
11. Badaut J, Lasbennes F, Magistretti PJ, Regli L. Aquaporins in brain: distribution, physiology, and pathophysiology. *J Cereb Blood Flow Metab* 2002;**22**:367–78.
12. Wen H, Nagelhus EA, Amiry-Moghaddam M, Agre P, Ottersen OP, Nielsen S. Ontogeny of water transport in rat brain: postnatal expression of the aquaporin-4 water channel. *Eur J Neurosci* 1999;**11**:935–45.
13. Nagelhus EA, Veruki ML, Torp R, et al. Aquaporin-4 water channel protein in the rat retina and optic nerve: polarized expression in Müller cells and fibrous astrocytes. *J Neurosci* 1998;**18**:2506–19.
14. Nagelhus EA, Horio Y, Inanobe A, et al. Immunogold evidence suggests that coupling of K+ siphoning and water transport in rat retinal Müller cells is mediated by a coenrichment of Kir4.1 and AQP4 in specific membrane domains. *Glia* 1999;**26**:47–54.
15. Manley GT, Fujimura M, Ma T, et al. Aquaporin-4 deletion in mice reduces brain edema after acute water intoxication and ischemic stroke. *Nat Med* 2000;**6**:159–63.
16. Verkman AS. Novel roles of aquaporins revealed by phenotype analysis of knockout mice. *Rev Physiol Biochem Pharmacol* 2005;**155**:31–55.
17. Vizuete ML, Venero JL, Vargas C, et al. Differential upregulation of aquaporin-4 mRNA expression in reactive astrocytes after brain injury: potential role in brain edema. *Neurobiol Dis* 1999;**6**:245–58.
18. Vajda Z, Promeneur D, Dóczi T, Sulyok E, et al. Increased aquaporin-4 immunoreactivity in rat brain in response to systemic hyponatremia. *Biochem Biophys Res Commun* 2000;**270**:495–503.
19. Ke C, Poon WS, Ng HK, Pang JC, Chan Y. Heterogeneous responses of aquaporin-4 in oedema formation in a replicated

severe traumatic brain injury model in rats. *Neurosci Lett* 2001;**301**:21–4.
20. Nico B, Frigeri A, Nicchia GP, et al. Severe alterations of endothelial and glial cells in the blood–brain barrier of dystrophic mdx mice. *Glia* 2003;**42**:235–51.
21. Saadoun S, Papadopoulos MC, Davies DC, Krishna S, Bell BA. Aquaporin-4 expression is increased in oedematous human brain tumours. *J Neurol Neurosurg Psychiatry* 2002;**72**:262–5.
22. Frigeri A, Gropper MA, Turck CW, Verkman AS. Immunolocalization of the mercurial-insensitive water channel and glycerol intrinsic protein in epithelial cell plasma membranes. *Proc Natl Acad Sci USA* 1995;**92**:4328–31.
23. Warth A, Kröger S, Wolburg H. Redistribution of aquaporin-4 in human glioblastoma correlates with loss of agrin immunoreactivity from brain capillary basal laminae. *Acta Neuropathol* 2004;**107**:311–8.
24. Warth A, Mittelbronn M, Wolburg H. Redistribution of the water channel protein aquaporin-4 and the K+ channel protein Kir4.1 differs in low- and high-grade human brain tumors. *Acta Neuropathol* 2005;**109**:418–26.
25. Warth A, Simon P, Capper D, et al. Expression pattern of the water channel aquaporin-4 in human gliomas is associated with blood–brain barrier disturbance but not with patient survival. *J Neurosci Res* 2007;**85**:1336–46.
26. Papadopoulos MC, Saadoun S, Verkman AS. Aquaporins and cell migration. *Pflugers Arch* 2008;**456**:693–700.
27. Ribatti D. The crucial role of vascular permeability factor/vascular endothelial growth factor in angiogenesis: a historical review. *Br J Haematol* 2005;**128**:303–9.
28. Nico B, Corsi P, Vacca A, Roncali L, Ribatti D. Vascular endothelial growth factor and vascular endothelial growth factor receptor-2 expression in mdx mouse brain. *Brain Res* 2002;**953**:12–6.
29. Nico B, Corsi P, Ria R, et al. Increased matrix-metalloproteinase-2 and matrix-metalloproteinase-9 expression in the brain of dystrophic mdx mouse. *Neuroscience* 2006;**140**:835–48.
30. Chaudhry IH, O'Donovan DG, Brenchley PE, Reid H, Roberts IS. Vascular endothelial growth factor expression correlates with tumour grade and vascularity in gliomas. *Histopathology* 2001;**39**:409–15.
31. Croll SD, Wiegand SJ. Vascular growth factors in cerebral ischemia. *Mol Neurobiol* 2001;**23**:121–35.
32. Rite I, Machado A, Cano J, Venero JL. Intracerebral VEGF injection highly upregulates AQP4 mRNA and protein in the perivascular space and glia limitans externa. *Neurochem Int* 2008;**52**:897–903.
33. Stupp R, Mason WP, van den Bent MJ, et al. Radiotherapy plus concomitant and adjuvant temozolomide for glioblastoma. *New Engl J Med* 2005;**352**:987–96.
34. Brandes AA, Tosoni A, Spagnolli F, et al. Disease progression or pseudoprogression after concomitant radiochemotherapy treatment: pitfalls in neurooncology. *Neurooncology* 2008;**10**:361–7.
35. Sawada T, Kato Y, Kobayashi M, Takekekawa Y. Immunohistochemical study of tight junction-related protein in neovasculature in astrocytic tumor. *Brain Tumor Pathol* 2000;**17**:1–6.
36. Bertossi M, Virgintino D, Maiorano E, Occhiogrosso M, Roncali L. Ultrastructural and morphometric investigation of human brain capillaries in normal and peritumoral tissues. *Ultrastruct Pathol* 1997;**21**:41–9.
37. Sinha S, Bastin ME, Wardlaw JM, Armitage PA, Whittle IR. Effects of dexamethasone on peritumoural oedematous brain: a DT-MRI study. *J Neurol Neurosurg Psychiatry* 2004;**75**:1632–5.
38. Heiss JD, Papavassiliou E, Merrill MJ, et al. Mechanism of dexamethasone suppression of brain tumor-associated vascular permeability in rats. Involvement of the glucocorticoid receptor and vascular permeability factor. *J Clin Invest* 1996;**98**:1400–8.
39. Gu YT, Zhang H, Xue YX. Dexamethasone treatment modulates aquaporin-4 expression after intracerebral hemorrhage in rats. *Neurosci Lett* 2007;**413**:126–31.
40. Hirt L, Ternon B, Price M, Mastour N, Brunet JF, Badaut J. Protective role of early aquaporin 4 induction against postischemic edema formation. *J Cereb Blood Flow Metab* 2008;**29**:423–33.
41. Zeynalov E, Chen CH, Froehner SC, et al. The perivascular pool of aquaporin-4 mediates the effect of osmotherapy in postischemic cerebral edema. *Crit Care Med* 2008;**36**:2634–40.
42. Olsen ML, Sontheimer H. Mislocalization of Kir channels in malignant glia. *Glia* 2004;**46**:63–73.
43. Saadoun S, Papadopoulos MC, Watanabe H, Yan D, Manley GT, Verkman AS. Involvement of aquaporin-4 in astroglial cell migration and glial scar formation. *J Cell Sci* 2005;**118**:5691–8.
44. Auguste KI, Jin S, Uchida K, et al. Greatly impaired migration of implanted aquaporin-4-deficient astroglial cells in mouse brain toward a site of injury. *FASEB J* 2007;**21**:108–16.
45. Giese A, Westphal M. Glioma invasion in the central nervous system. *Neurosurgery* 1996;**39**:235–50.
46. Zhou D, Jiang X, Xu R, et al. Assessing the cytoskeletal system and its elements in C6 glioma cells and astrocytes by atomic force microscopy. *Cell Mol Neurobiol* 2008;**28**:895–905.
47. Takekawa Y, Sawada T. Vascular endothelial growth factor and neovascularization in astrocytic tumors. *Pathol Int* 1998;**48**:109–14.
48. Sundberg C, Nagy JA, Brown LF, et al. Glomeruloid microvascular proliferation follows adenoviral vascular permeability factor/vascular endothelial growth factor-164 gene delivery. *Am J Pathol* 2001;**158**:1145–60.
49. Fischer I, Gagner JP, Law M, Newcomb EW, Zagzag D. Angiogenesis in gliomas: biology and molecular pathophysiology. *Brain Pathol* 2005;**15**:297–310.
50. Sawada T, Kato Y, Kobayashi M. Expression of aquaporin-4 in central nervous system tumors. *Brain Tumor Pathol* 2007;**24**:81–4.
51. Winkler F, Kozin SV, Tong RT, et al. Kinetics of vascular normalization by VEGFR-2 blockade governs brain tumor response to radiation: role of oxygenation, angiopoietin-1, and matrix metalloproteinases. *Cancer Cell* 2004;**6**:553–63.